

Determination of Flutamide Toward Real-Time Electrochemical Sensor Based on Ultrathin Reduced Graphene Oxide Covered MoW-P

Naveen Karuppusamy ^a, Srinithi Subburaj^a, Shen Ming Chen ^{a*}, Pitchaimani Veerakumar ^b, Kuan-Yu Lin ^a, S. Meenakshi ^c.

^a Department of Chemical Engineering and Biotechnology, National Taipei University of Technology, No.1, Section 3, Chung-Hsiao East Road, Taipei 106, Taiwan.

^b Department of Biochemistry, Saveetha Dental College and Hospitals, 162, Poonamallee High Road, Velappanchavadi, Chennai, Tamil Nadu, India-600077.

^c Department of Chemistry, SRM Institute of Science and Technology, Ramapuram Campus, Chennai, Tamil Nadu, India-600089

Corresponding author: S.M. Chen,

Email: smchen1957@gmail.com, smchen78/ms15.hinet.net,

Tel: +886 2270 17147, Fax: +886 2270 25.

Material Characterization

The crystalline phase of prepared sample analyzed with XRD spectra acquired using Cu-K α radiation ($\lambda = 1.54 \text{ \AA}$) on XPERT-PRO PANalytical instruments. The Field emission scanning electron microscope (FE-SEM) and High-resolution transmission electron microscope (HR-TEM) images of material taken using HITACHI S-3000H with energy dispersive X-ray (EDX) for the elemental mapping and JEM-1200 EX at the acceleration of 200 kV coupled with HORIBA EMAX X-ACT for EDX elemental mapping. Perkin-Elmer IR spectroscopy used for the Functional group identification in the sample from the FT-IR band. The valence state of elements and the metal coordination presents in material identified by the XPS spectra obtained from Thermo ESCALAB instrument. The Brunauer–Emmett–Teller (BET) adsorption-desorption curve obtained from the Micromeritics ASAP-2020A instrument used to measure the surface area and the pore volume of the samples.

Electrochemical measurements

As prepared RGO, MoW-P and MoW-P/RGO catalyst loaded on the surface of GCE as a working electrode for its comparative study and tested its electrochemical performance on a three-electrode cell containing PBS (N_2 saturated) as electrolyte towards FLT with the electrochemical workstation for cyclic voltammetry (CHI1205B) & for differential pulse voltammetry (CHI900) comprised of 3M KCl saturated Ag/AgCl electrode and platinum wire are used as a reference, counter electrode respectively.

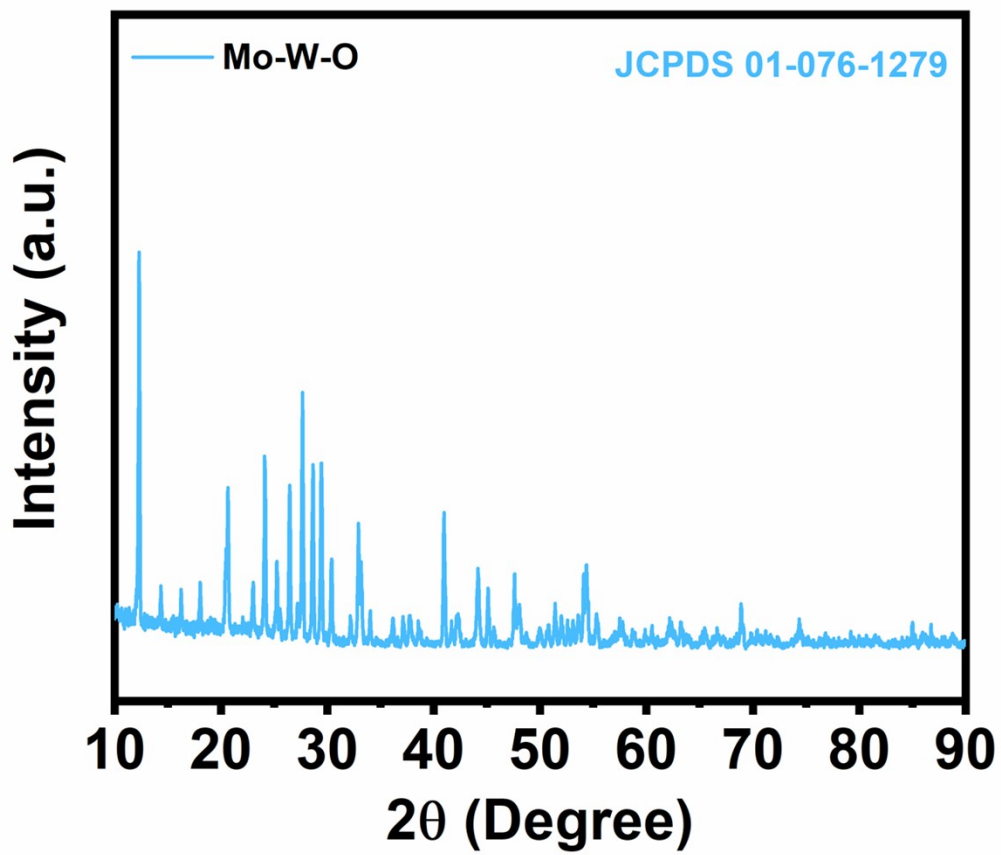


Fig. S1. XRD pattern of Mo-W-O.

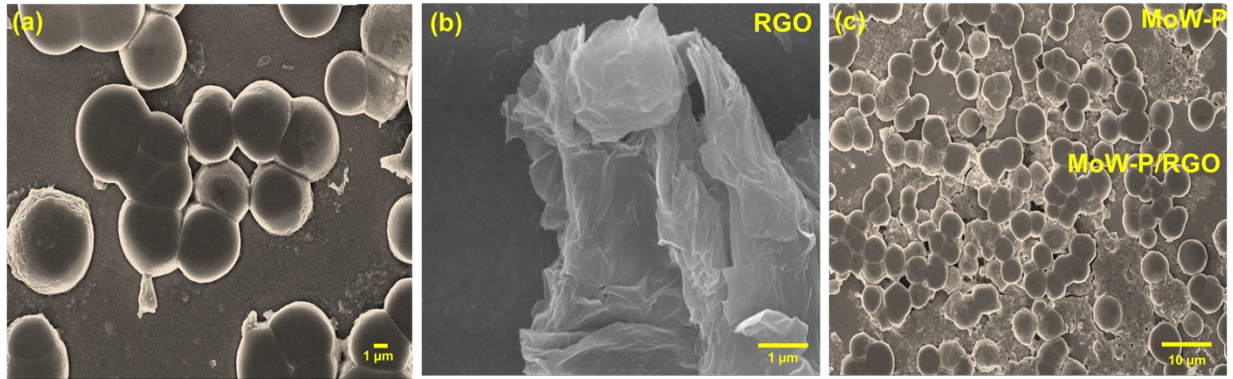


Fig. S2. FE-SEM images of MoW-P, RGO, and MoW-P/RGO.

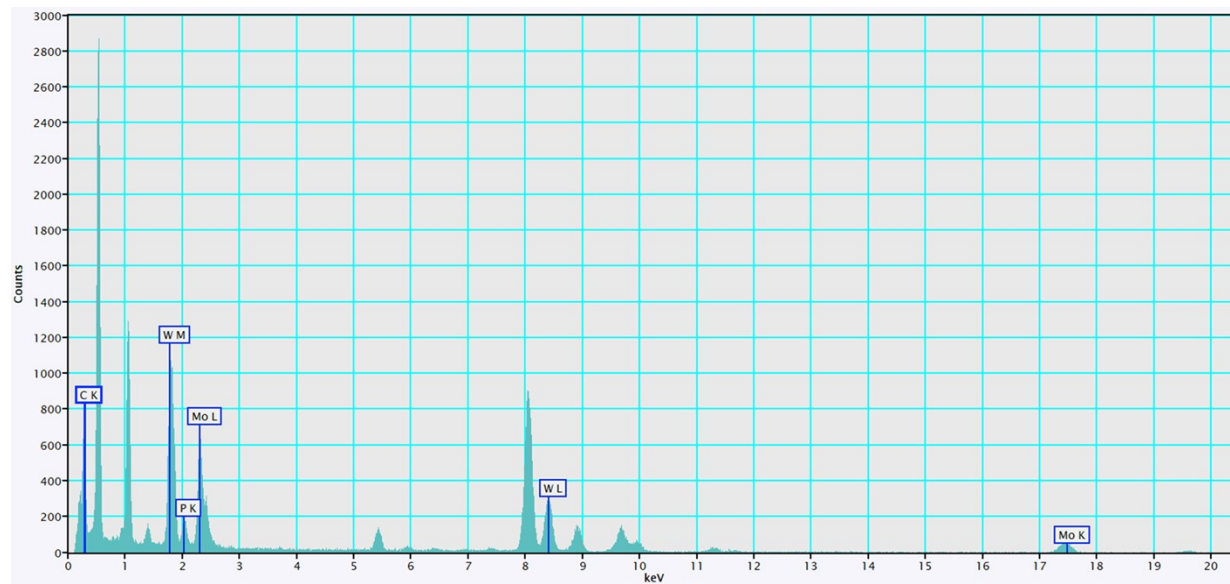


Fig. S3. EDX spectrum of MoW-P/RGO composite observed from the HR-TEM image.

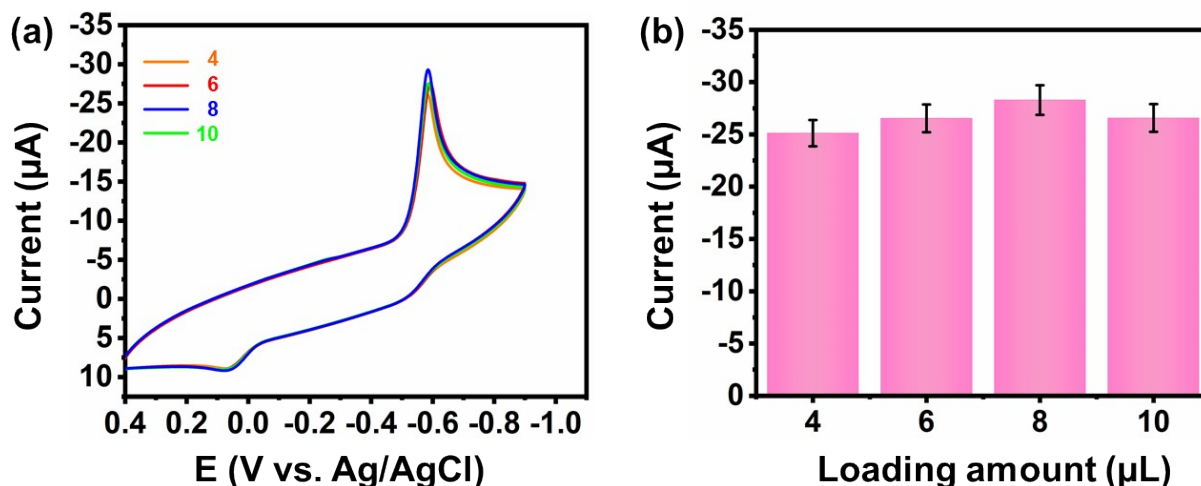


Fig. S4. (a) MoW-P@RGO/GCE tested by varying the loading amount with the addition of 100 μM FLT to the 0.1 M PBS, and (b) the relative current response represents in a bar graph.

Optimization Studies

The amount of electrocatalyst coated on GCE also affects the current responses in either way of lowering or increasing response depending on the amount of catalyst. To optimize the loading amount of prepared electrocatalyst tested with CV by changing loading amount (4, 6, 8 & 10 μL) with the addition of 100 μM of FLT to the PB electrolyte. In **Fig. S4a**, the current response of MoW-P/RGO/GCE proportionally increases up to 8 μL loading amount, and at 10 μL of loading the current tends to decrease as shown in bar graph **Fig. S4b**, due to the higher concentration of electrocatalyst blocks the surface of GCE which decrease the number of electron transfer. So, 8 μL of electrocatalyst was chosen as an optimized amount and performed the electrochemical investigations.

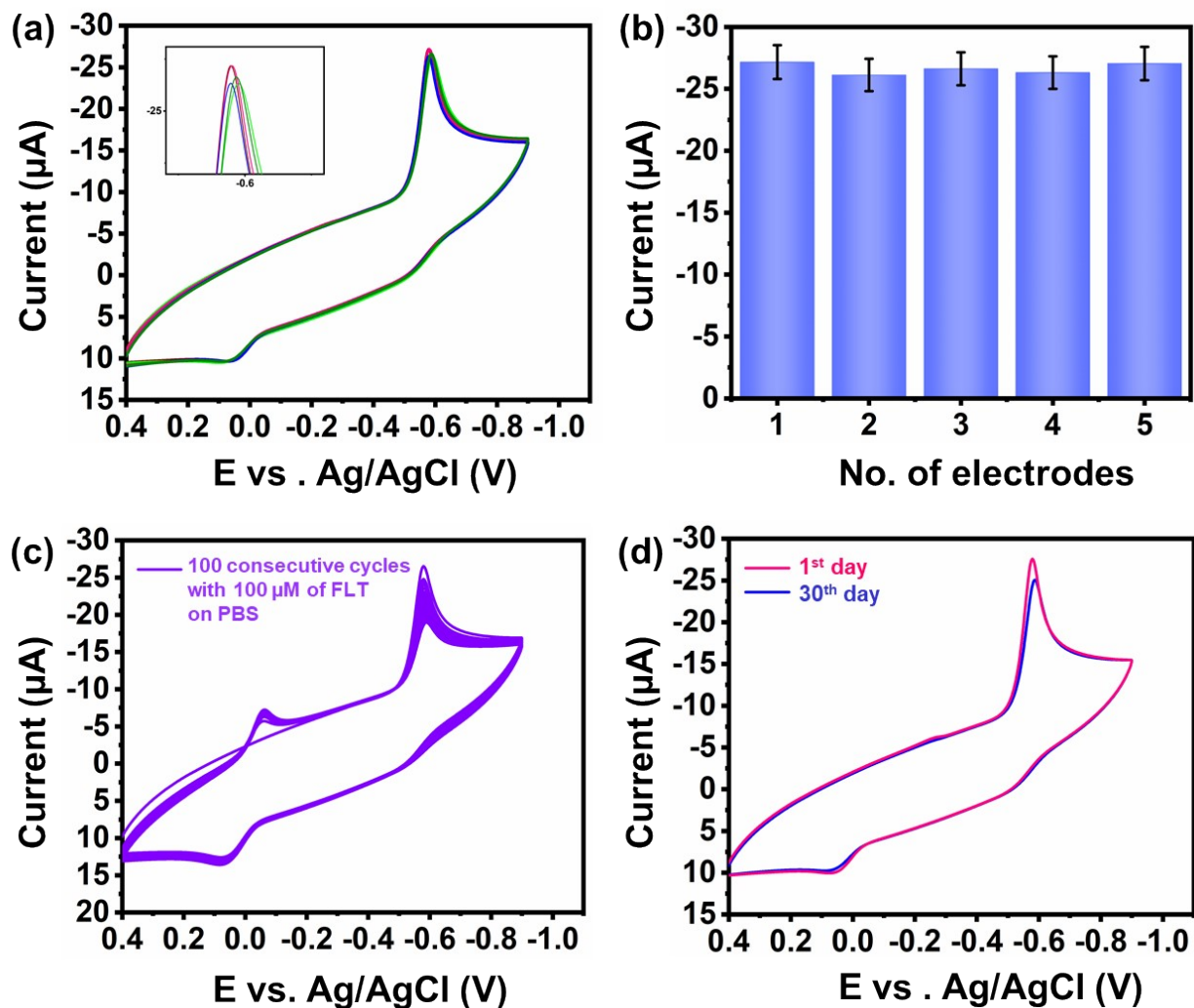


Fig. S5. (a) CV response, (b) the relative current bar graph from five independent GCE modified using MoW-P@RGO with 100 μM FLT to the 0.1 M PBS, (c) 100 consecutive cycle and (d) the stability of MoW-P@RGO tested with 100 μM FLT to the 0.1 M PBS.

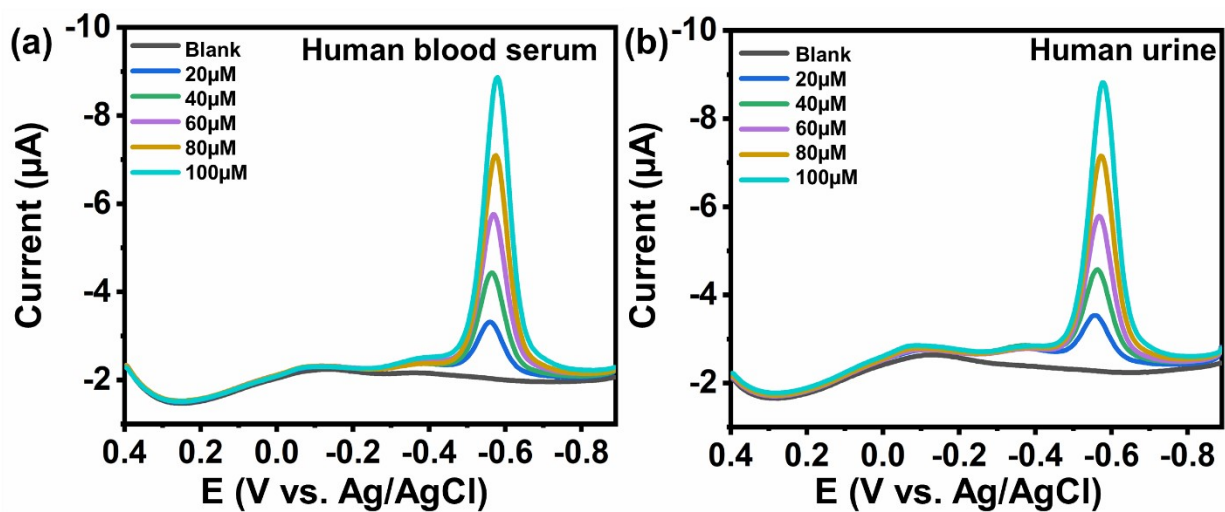


Fig.S6. DPV response for FLT in (a) human blood serum and (b) human urine samples in presence of possible interfering compound such as ascorbic acid, dopamine, uric acid, and glucose molecules.

| Electrode | Method | LOD (μM) | Linear range (μM) | Sensitivity ($\mu A \mu M^{-1} cm^{-2}$) | Reference |
|----------------------------------|------------------|--------------------|-----------------------------|---|-----------|
| MXene/(MOF(ZIF-67) | ^b DPV | 0.015 | 0.05 - 70 | - | [S1] |
| BiVO ₄ -rGO/CE-BN/GCE | DPV | 0.011 | 0.04–1236.2 | 3.80 | [S2] |
| MnFeZn-LDH | DPV | 0.012 | 0.019-2735.7 | 5.04 | [S3] |
| Au/GCE | DPV | 0.0015 | 1–600 | - | [S4] |
| Sn-ZnO/RGO | DPV | 0.0073 | 0.01–170 | 14.10 | [S5] |
| ^a FCO/PPy/SPCE | DPV | 0.086 | 0.4–376 | 1.45 | [S6] |
| FeVO ₄ -150 | DPV | 0.054 | 0.06–777.46 | - | [S7] |
| MoW-P@RGO | DPV | 0.009 | 0.3-1152 | 0.502 | This work |

Table.S1 Comparison of various reported FLT sensor with the MoW-P/RGO composite.

a- iron-cobalt oxide/polypyrrole/screen printed carbon electrode; b- Differential pulse voltammetry; c- Square Wave Cathodic Adsorptive Stripping Voltammetry.

Table.S2 Real sample performance on human blood serum and human urine sample with the

| Sample | Added amount [μM] | Detected amount [μM] | Recovery (%) | RSD (%) |
|------------------------------|--|---|-------------------------|--------------------|
| | 0 | - | - | - |
| Human blood serum | 10 | 9.78 | 97.8 | 2.99 |
| | 20 | 18.40 | 92.0 | 2.85 |
| | 30 | 28.10 | 93.6 | 2.97 |
| | 0 | - | - | - |
| Human urine | 10 | 9.44 | 94.4 | 2.90 |
| | 20 | 18.1 | 90.5 | 3.01 |
| | 30 | 28.34 | 94.4 | 3.20 |

MoW-P/RGO composite.

Number of measurements, n=3.

Table S3. Real sample performance on human blood serum and human urine sample with the MoW-P/RGO composite with the presence of possible interfering compound such as ascorbic acid, dopamine, uric acid, and glucose molecules.

| Sample | Added amount [μM] | Detected amount [μM] | Recovery (%) | RSD (%) |
|------------------------------|--|---|-------------------------|--------------------|
| Human blood serum | Blank | - | - | - |
| | 20 | 18.75 | 93.75 | 1.57 |
| | 40 | 38.29 | 95.72 | 1.55 |
| | 60 | 57.68 | 96.13 | 1.60 |
| | 80 | 78.20 | 97.75 | 1.48 |
| | 100 | 98.87 | 98.87 | 1.23 |
| Human urine | Blank | - | - | - |
| | 20 | 19.62 | 98.10 | 1.80 |
| | 40 | 38.48 | 96.20 | 1.88 |
| | 60 | 58.45 | 97.41 | 1.79 |
| | 80 | 77.88 | 97.35 | 1.80 |
| | 100 | 97.03 | 97.03 | 1.82 |

Number of measurements, n=3.

Reference

- S1 Y. Li, L. Zhang, M. Wu, G. Ma, M. Motlak and A. Mahdi, *Inorg. Chem. Commun.*, 2023, 111061.
- S2 C. Bhuvaneswari, K. Palpandi, B. Amritha, P. Paunkumar, R. L. Priya, N. Raman and S. G. Babu, *Microchem. J.*, 2023, **184**, 108174.
- S3 S. Tharuman, N. Nataraj, S.-M. Chen, V. Sasirekha and C. Ragumoorthy, *Surfaces and Interfaces*, 2023, 103195.
- S4 A. Mehrabi, M. Rahimnejad, M. Mohammadi and M. Pourali, *J. Appl. Electrochem.*, 2021, **51**, 597–606.
- S5 K. Y. Hwa, A. Santhan and S. K. S. Tata, *Microchem. J.*, 2021, **160**, 105689.
- S6 N. Manjula, V. Vinothkumar and S. M. Chen, *Colloids Surfaces A Physicochem. Eng. Asp.*, 2021, **628**, 127367.
- S7 G. Kesavan, M. Pichumani and S. M. Chen, *ACS Appl. Nano Mater.*, 2021, **4**, 5883–5894.